

# Accessing Unusual Reactivity through Chelation-Promoted Bond Weakening

Nicholas G. Boeckell, Caroline O. Bartulovich, Sandeepan Maity, and Robert A. Flowers, II\*



Cite This: *Inorg. Chem.* 2023, 62, 5040–5045



Read Online

ACCESS |



Metrics & More

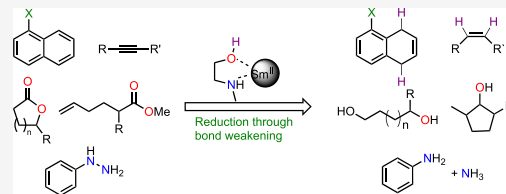


Article Recommendations



Supporting Information

**ABSTRACT:** Highly reducing Sm(II) reductants and protic ligands were used as a platform to ascertain the relationship between low-valent metal-protic ligand affinity and degree of ligand X–H bond weakening with the goal of forming potent proton-coupled electron transfer (PCET) reductants. Among the Sm(II)-protic ligand reductant systems investigated, the samarium dibromide *N*-methylethanolamine (SmBr<sub>2</sub>-NMEA) reagent system displayed the best combination of metal–ligand affinity and stability against H<sub>2</sub> evolution. The use of SmBr<sub>2</sub>-NMEA afforded the reduction of a range of substrates that are typically recalcitrant to single-electron reduction including alkynes, lactones, and arenes as stable as biphenyl. Moreover, the unique role of NMEA as a chelating ligand for Sm(II) was demonstrated by the reductive cyclization of unactivated esters bearing pendant olefins in contrast to the SmBr<sub>2</sub>-water-amine system. Finally, the SmBr<sub>2</sub>-NMEA reagent system was found to reduce substrates analogous to key intermediates in the nitrogen fixation process. These results reveal SmBr<sub>2</sub>-NMEA to be a powerful reductant for a wide range of challenging substrates and demonstrate the potential for the rational design of PCET reagents with exceptionally weak X–H bonds.

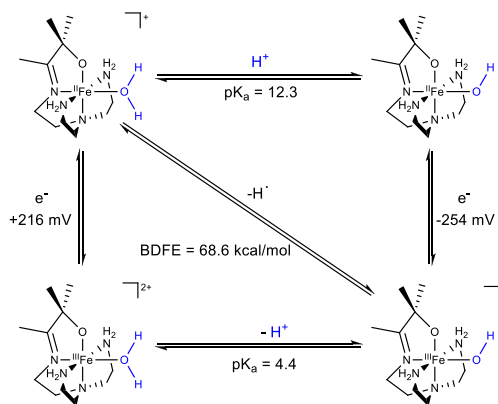


## INTRODUCTION

The coordination of a Lewis basic ligand containing X–H bonds (where X = O, N, etc.) to a redox-active metal in a higher oxidation state leads to a substantial heterolytic weakening of the coordinated ligand producing a stronger acid. However, coordination to the same metal in a lower oxidation state has a less profound impact on the acidity of the coordinated ligand. Conversely, coordination of ligands with X–H bonds to low-valent metals leads to a significant decrease in the ligand bond dissociation energy.<sup>1</sup> This unique feature of ligand coordination to a redox-active center is best exemplified by the work of Kovacs and colleagues shown in Scheme 1. The pK<sub>a</sub> of water coordinated to the iron(II) complex I is 8 orders of magnitude less acidic than coordination to the iron(III) analogue III. However, coordination of water to I leads to a bond weakening of the O–H of approximately 54 kcal/mol.<sup>2</sup>

There are a number of other examples of bond weakening that demonstrate the impact of coordination to low-valent metals through coordination of protic ligands.<sup>3–5</sup> An impressive example by Peters and co-workers established that the protonation of Cp\*<sub>2</sub>Co and related low-valent metallocenes leads to the formation of an incredibly weak C–H or N–H bond. These reagents enable formal hydrogen atom transfer (HAT) that provides a unique approach for the development of proton-coupled electron transfer (PCET) donors and PCET mediators in a number of reductions and bond-forming reactions.<sup>6–8</sup> While all of the aforementioned examples provide strategies to induce bond weakening, the use of this approach in synthesis is only being fully realized,

## Scheme 1. Thermochemical Square for the Dehydrogenation of I<sup>2</sup>

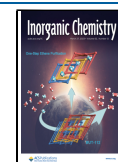


predominantly through the work of Knowles and co-workers.<sup>9–11</sup>

Over the past several years, we have explored the mechanism of reactions that use the combination of samarium diiodide (SmI<sub>2</sub>) and water. This reagent system is unusual since it

Received: January 29, 2023

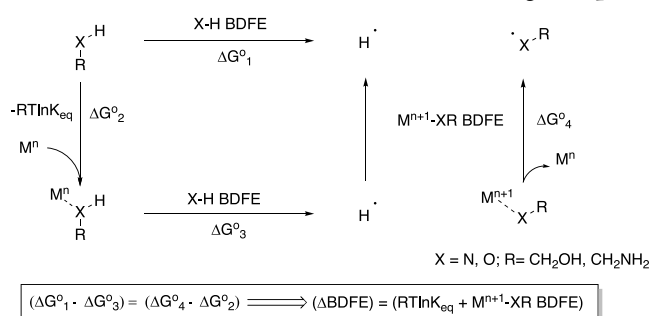
Published: March 13, 2023



facilitates the reduction of substrates that have significantly more negative reduction potentials than the Sm(II)-water complex.<sup>11</sup> The work of our group and that of Mayer and Kolmar provide compelling evidence that the reduction of many substrates by SmI<sub>2</sub>-water proceeds through proton-coupled electron transfer (PCET).<sup>12–14</sup> While the use of Sm(II)-water in synthesis is well documented,<sup>15</sup> it can also be employed in other systems as exemplified by the elegant work of Nishibayashi et al., demonstrating that the reagent system can be used to reduce nitrogen through molybdenum-catalyzed fixation.<sup>16</sup>

Recently, we proposed that a key feature responsible for the unique reactivity of the Sm(II)-water complex is strong coordination that leads to significant weakening of the O–H bond of ligated water.<sup>17</sup> If this supposition is correct, then the stronger the coordination between a low-valent metal and ligand, the greater the degree of bond weakening that should occur. The thermochemical cycle in Scheme 2 provides a

### Scheme 2. Thermochemical Cycle for Metal–Ligand Association and H-Atom Loss from the Resulting Complex<sup>4</sup>



thermodynamic argument in favor of this point, demonstrating that the change in the bond dissociation free energy (BDFE) will be greater for ligands that have a strong interaction with a low-valent metal.<sup>4</sup> The cycle in Scheme 2 shows that the energy difference between the X–H bond strength of the free ( $\Delta G^{\circ}_1$ ) and low-valent metal-bound ligand ( $\Delta G^{\circ}_3$ ) is equal to the energy difference between the  $M^{n+1}$ -XR BDFE ( $\Delta G^{\circ}_4$ ) and the free energy of coordination between the chelating ligand RX–H and  $M^n$  ( $\Delta G^{\circ}_2$ ). Since all free energy terms are positive, the  $\Delta \text{BDFE}$  (X–H bond weakening) will be greater for high affinity ligands. In addition, the Coulombic affinity between the deprotonated ligand and the high valent metal provides an additional important driving force.

Reagents based on Sm(II) provide a unique platform to test this supposition because a range of anionic ligands can be readily exchanged to tune the redox potential of the reagent, and the large coordination sphere enables the coordination of a variety of protic ligands. Furthermore, Lewis basic ligands such as glycols and amino alcohols that coordinate with varying affinities to Sm(II) are easily accessible. Herein, we demonstrate that the appropriate choice of chelating the protic Lewis base and Sm(II) reductant can be identified that combines complex stability and reactivity, enabling the reduction of a range of substrates through PCET that cannot be reduced by electron transfer alone.

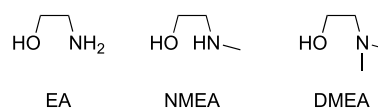
## RESULTS AND DISCUSSION

To initially examine the relationship between protic ligand affinity for Sm(II) and reactivity, a series of strongly reducing

Sm(II) complexes in THF were examined including samarium dibromide (SmBr<sub>2</sub>), samarium dichloride (SmCl<sub>2</sub>), decamethyl samarocene (SmCp\*<sub>2</sub>), and Sm(II) *bis*-trimethylsilyl amide (Sm(HMDS)<sub>2</sub>).<sup>18–20</sup> Addition of 15 equiv of ethylene glycol and ethanolamine with respect to [Sm(II)] was initiated for each reductant in a sealed round bottom flask under an Ar atmosphere, and the evolution of H<sub>2</sub> was monitored via a pressure sensor over 10 min. Most combinations evolved H<sub>2</sub> too rapidly to be useful, but among those examined, SmBr<sub>2</sub> and ethanolamine provided the most stable combination of reagents.

We have previously demonstrated that the steric bulk of an alcohol impacts the affinity for Sm(II).<sup>21</sup> To determine whether the affinity of an ethanolamine for Sm(II) could be further modulated, a series of ligands including ethanolamine (EA), *N*-methylethanolamine (NMEA), and *N,N*-dimethylethanolamine (DMEA) shown in Scheme 3 were examined using UV–vis spectrophotometry.

### Scheme 3. Ethanolamines Used in the Study



As predicted, EA had the highest affinity for SmBr<sub>2</sub> in THF followed by NMEA and DMEA as measured by UV–vis spectroscopy (see the Supporting Information). Although EA had the highest affinity for SmBr<sub>2</sub>, it was the least stable among the series. The combination of SmBr<sub>2</sub>-NMEA (shown in Figure 1) was the most promising since it had a high affinity for the metal and was stable within a reasonable timeframe for further reactivity studies.

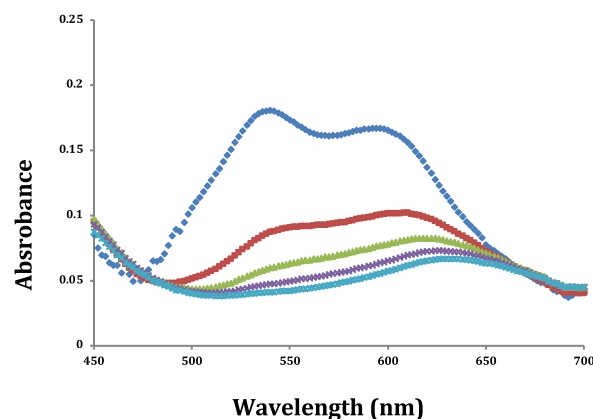


**Figure 1.** UV–vis absorption spectra of 2 mM SmBr<sub>2</sub> (blue diamond) in the presence of 5 equiv (red solid square), 10 equiv (green open square), 15 equiv (purple open square), and 20 equiv (blue open square) of NMEA.

Next, conductance studies were performed to elucidate the nature of the SmBr<sub>2</sub>-ethanolamine complexes formed in solution. Addition of strongly coordinating ligands to samarium dihalides induces full or partial halide dissociation, which can be detected via the corresponding increase in solution conductivity. Based on the previous UV–vis studies, we predicted that EA would induce the greatest degree of bromide displacement from Sm(II) followed by NMEA and DMEA. However, the solution conductivity data shown in

Figure 2 is consistent with the greatest degree of bromide displacement upon addition of NMEA to  $\text{SmBr}_2$  followed by

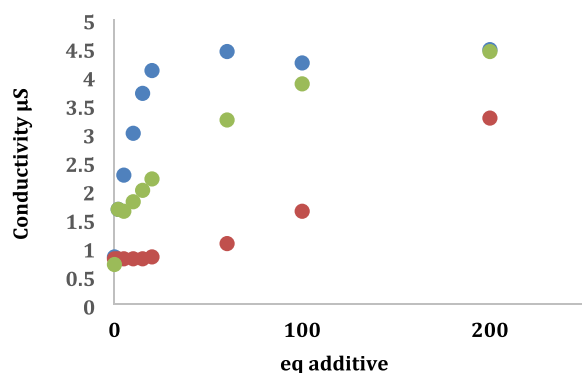
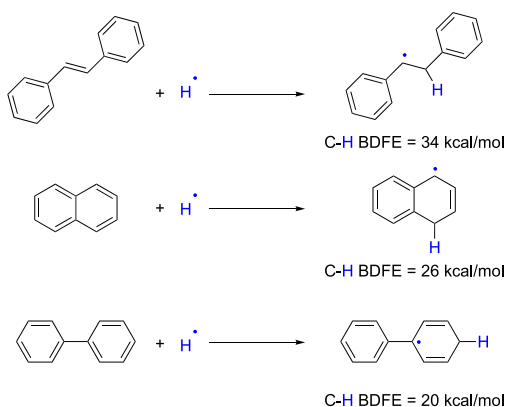


**Figure 2.** Conductivity study of  $\text{SmBr}_2$  in the presence of different ligands EA (red circles), NMEA (blue circles), and DMEA (green circles).

DMEA and EA. These results suggest that the steric bulk of the high-affinity ligand also plays a significant role in inducing halide displacement upon coordination to  $\text{SmBr}_2$ . Based on the UV–vis affinity data in Figure 1 and the solution conductivity data in Figure 2, we propose that the combination of the high affinity of NMEA for  $\text{Sm(II)}$  coupled with the steric bulk afforded by an *N*-methyl group is responsible for the observed degree of bromide displacement from  $\text{Sm(II)}$  upon coordination of NMEA.

To assess the reactivity of the  $\text{SmBr}_2$ -NMEA reagent system and test the limits of reduction, a series of arenes were examined that form successively weaker C–H bonds upon formal hydrogen atom transfer (HAT), as shown in Scheme 4

#### Scheme 4. Products of Initial HAT Reductions of Arenes by $\text{SmBr}_2$ -NMEA and Associated C–H BDFEs

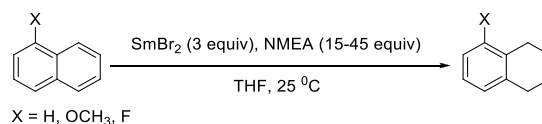


(see the Supporting Information).<sup>22</sup> This approach enables an estimation of the degree of bond weakening that occurs upon coordination of NMEA to  $\text{SmBr}_2$  since the initial HAT from the complex could be endergonic by 5–10 kcal/mol followed by subsequent ET-PT or PCET exergonic steps. All arenes were reduced by  $\text{SmBr}_2$ -NMEA in THF rapidly at room temperature. *trans*-Stilbene and naphthalene provided clean reductions, while the reduction of biphenyl produced several products including cyclohexylbenzene.

Since the reduction of naphthalene proceeded cleanly, this framework was chosen for further studies. Both 1-methox-

naphthalene and 1-fluoronaphthalene were reduced to the 1,4-dihydronaphthalene products by  $\text{SmBr}_2$  containing 4–15 equiv of NMEA (based on  $[\text{SmBr}_2]$ ), as shown in Figure 3A.

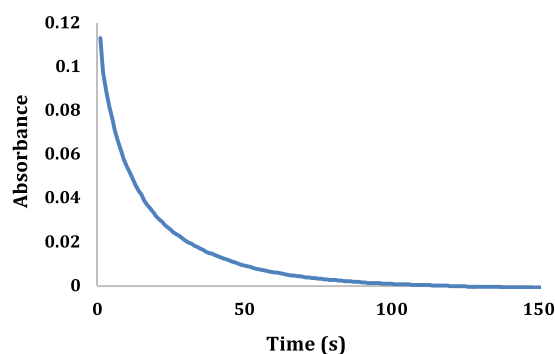
#### A. Reduction of naphthalene derivatives by $\text{SmBr}_2$ -NMEA



entry <sup>a</sup>	substrate	yield (%)
1	naphthalene	90 <sup>b</sup>
2	1-methoxynaphthalene	96 <sup>b</sup>
3	1-fluoronaphthalene	90 <sup>c</sup>

<sup>a</sup>Conditions: 3 equiv  $\text{SmBr}_2$ , 4–15 equiv NMEA, rt, 12 h. <sup>b</sup>isolated yield <sup>c</sup>NMR yield, the balance of the reaction provided the defluorinated product.

#### B. Sample decay curve for 0.15 M NMEA, 90 mM 1-methoxynaphthalene, and 10 mM $\text{SmBr}_2$ at 25 °C.



Component	Rate Order	$\Delta H^\ddagger$ , d,e (kcal/mol)	$\Delta S^\ddagger$ , d,e (cal/mol K)	$\Delta G^\ddagger$ , d,f (kcal/mol)
$\text{SmBr}_2$	1 <sup>a</sup>			
2	1.0 ± 0.1 <sup>b</sup>	9.2 ± 0.2	-34 ± 2	19.3 ± 0.3
NMEA	0.8 ± 0.1 <sup>c</sup>			

<sup>a</sup>Fractional times method. <sup>b</sup>10 mM  $\text{SmBr}_2$ , 60–100 mM 2, 150 mM NMEA. <sup>c</sup>10 mM  $\text{SmBr}_2$ , 100 mM 2, 50–250 mM NMEA. <sup>d</sup>Conditions: 10 mM  $\text{SmBr}_2$ , 100 mM 2, 150 mM NMEA. The activation parameters are the averages of three independent experiments from 15 to 35 °C and are reported as ± σ. <sup>e</sup>Obtained from  $\ln(k_{\text{obs}}/k_B T) = \Delta H^\ddagger/RT + \Delta S^\ddagger/R$ . <sup>f</sup>Calculated from  $\Delta G^\ddagger = \Delta H^\ddagger - T\Delta S^\ddagger$  at 25 °C.

**Figure 3.** (A, B) Kinetic studies of substrate reduction by  $\text{SmBr}_2$ -NMEA.

Given the moderate rate of reduction of 1-methoxynaphthalene by  $\text{SmBr}_2$ -NMEA, it was identified as an ideal substrate for kinetic studies to examine the mechanism of arene reduction by  $\text{SmBr}_2$ -NMEA. Stopped-flow spectrophotometry was used to determine the rate of the reaction and the rate order of each component by monitoring the decay of the characteristic absorption of  $\text{Sm(II)}$  at 540 nm.<sup>23</sup> The results of these kinetic studies and a sample decay curve are shown in Figure 3B.

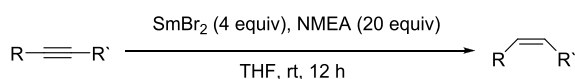
The results of the kinetic studies reveal that the reaction is approximately first order in each component with a rate constant of 4.9 M<sup>-2</sup> s<sup>-1</sup> for the reduction of 1-methoxynaphthalene by  $\text{SmBr}_2$ -NMEA at room temperature. Rate measurements using *N*- and *O*-deuterated NMEA provided a kinetic

isotope effect of 1.2. Activation parameters demonstrate a low barrier to bond reorganization and an organized transition state. Taken together, these data are consistent with previous studies of Sm(II)-proton donor systems where substrate reduction occurs through concerted proton–electron transfer (CPET).<sup>14</sup>

Previous collaborative work from our group demonstrated that Sm(II) is more azaphilic than oxophilic.<sup>24</sup> The presence of nitrogen in NMEA is likely responsible for the strong coordination between the ligand and metal. One question that remains is does H-transfer originate from the N–H or O–H bond? First, a previous study demonstrates that proton-transfer in arene reduction occurs from DMEA, a chelating ligand with no coordinated N–H bond.<sup>24</sup> Second, ethylenediamine, which is expected to coordinate more strongly, does not lead to substrate reduction.<sup>24</sup> Finally, substitution on the N or O of coordinating alcohols and amines inhibits coordination to Sm(II).<sup>4,21,24</sup> As a consequence, while nitrogen coordination enhances chelation to Sm(II), the more acidic proton from the bound O–H of NMEA is the likely source of hydrogen in substrate reduction.

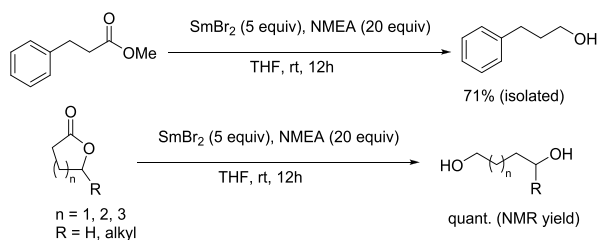
With this analysis in hand, we examined a series of substrates that are typically recalcitrant to ET from Sm(II). Three alkynes, 6-dodecyne, 5-decyne, and 4-decyne, were reduced to the *cis* products in 92, 88, and 58% yields, respectively, as shown in Scheme 5 below. The balance of each reaction was an unreduced starting material and a small amount of alkane.

**Scheme 5. Reaction Scheme for the Reductions of Alkynes to *cis*-Alkenes by SmBr<sub>2</sub>-NMEA**



The reduction of unactivated esters by SmBr<sub>2</sub>-NMEA was also examined. Methyl 3-phenylpropanoate,  $\gamma$ -heptalactone,  $\delta$ -decalactone, and  $\epsilon$ -caprolactone were each reduced quantitatively by a slight excess of SmBr<sub>2</sub>-NMEA to the respective alcohol and diol products shown in Scheme 6. While the

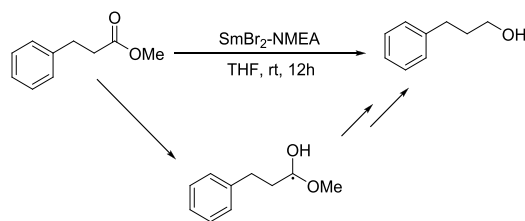
**Scheme 6. Reaction Scheme for the Reductions of Esters and Lactones by SmBr<sub>2</sub>-NMEA**



reductions of unactivated esters by SmI<sub>2</sub>-water-amine and six-membered lactones by SmI<sub>2</sub>-water are known, five- and seven-membered lactones are significantly more recalcitrant to reduction by Sm(II).<sup>25–28</sup>

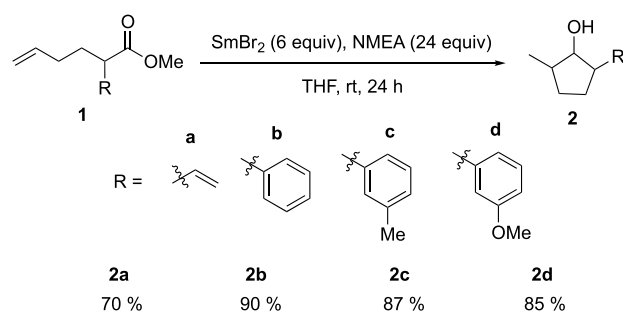
Building upon previous studies of ester reductions by Sm(II) reagents, it was hypothesized that ester reduction by SmBr<sub>2</sub>-NMEA proceeds through a C-centered radical intermediate, as shown in Scheme 7.<sup>29</sup> It was therefore proposed that the reduction of an unactivated ester with a pendant radicophile by SmBr<sub>2</sub>-NMEA should result in substrate cyclization. To test this supposition, we used an unactivated double bond as the

**Scheme 7. Reaction Scheme and Proposed Intermediate for the Reduction of Hydrocinnamic Methyl Ester by SmBr<sub>2</sub>-NMEA**



radicophile. Although an example of a cyclization of an ester with an activated double bond was recently demonstrated,<sup>30</sup> activated double bonds are often reduced preferentially to carbonyls by strong reductants and HAT reagents.<sup>31–33</sup> Gratifyingly, treatment of the family of ester-olefin substrates shown in Scheme 8 with SmBr<sub>2</sub>-NMEA resulted in substrate 5-

**Scheme 8. Reaction Scheme and Substrate Scope for the Reductive Cyclization of Ester-Olefins by SmBr<sub>2</sub>-NMEA**



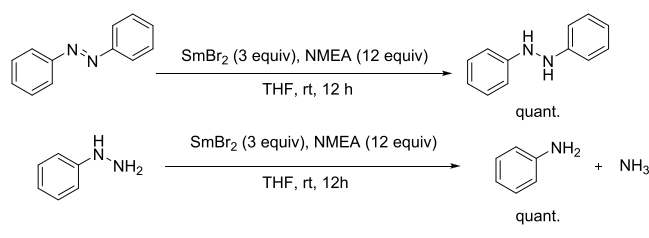
*exo*-trig radical cyclization to form the corresponding five-membered cyclic alcohols in very good to excellent isolated yields. The cyclic alcohol products each contain three stereocenters, and <sup>1</sup>H and <sup>13</sup>C NMR data collected for the products are consistent with the presence of multiple diastereomers. Although four diastereomers are possible, NMR spectra indicated the presence of two different diastereomers of equal distribution but we were unable to fully resolve stereoselectivity for this cyclization.

One question that arises from this work is whether the use of SmBr<sub>2</sub>-NMEA is mechanistically distinct from the Sm(II)-water-Et<sub>3</sub>N system developed by Hilmersson et al.<sup>34</sup> To test this question, **1d** was treated with SmBr<sub>2</sub>-water-Et<sub>3</sub>N, yielding a mixture of products and unreacted starting material. This result contrasts with the recovery of only the cyclized product **2d** from the reaction of **1d** with SmBr<sub>2</sub>-NMEA (see the Supporting Information). These observations are consistent with a difference in the mechanistic pathway between the ET-PT proposed for Sm(II)-water-Et<sub>3</sub>N compared to SmBr<sub>2</sub>-NMEA, which was demonstrated to proceed via PCET *vide supra*.<sup>35,36</sup>

Given the successful reduction of a broad scope of challenging substrates by SmBr<sub>2</sub>-NMEA, we considered whether the SmBr<sub>2</sub>-NMEA reagent could be applied to difficult substrate reductions of significant societal importance. Notably, the use of Sm(II)-water as a terminal reductant in the Mo-catalyzed fixation of N<sub>2</sub> has been described by Nishibayashi and co-workers.<sup>16</sup> We therefore investigated the reduction of analogues to intermediates in the nitrogen fixation process using SmBr<sub>2</sub>-NMEA. Azobenzene was found to be reduced

rapidly to give a quantitative yield of 1,2-diphenylhydrazine, as shown in Scheme 9 (top). The stability of the N–N  $\sigma$ -bond

**Scheme 9.** Reaction Schemes for the Reductions of Azobenzene and Phenylhydrazine by SmBr<sub>2</sub>-NMEA



against reduction by SmBr<sub>2</sub>-NMEA was hypothesized to be a consequence of steric interference by the two *N*-phenyl groups present in the substrate. Gratifyingly, reduction of phenylhydrazine to a quantitative yield of aniline by SmBr<sub>2</sub>-NMEA proceeded rapidly, as shown in Scheme 9 (bottom) with ammonia likely constituting the remainder of the product material.

## CONCLUSIONS

We have utilized the thermodynamic relationship between low-valent metal-protic ligand affinity and complex X–H BDFE to design the powerful PCET reductant SmBr<sub>2</sub>-NMEA. Subsequently, the SmBr<sub>2</sub>-NMEA reagent was shown to reduce a range of arenes as challenging as biphenyl and afforded facile conversion of alkynes to *cis*-alkenes. Moreover, SmBr<sub>2</sub>-NMEA mediated the rapid reduction of unactivated esters including five-, six-, and seven-membered lactones to their respective primary alcohols and diols. The intermediacy of the C-centered radical shown in Scheme 5 in the reduction of esters by SmBr<sub>2</sub>-NMEA was leveraged to afford 5-*exo*-trig cyclization of a family of unactivated ester-olefin substrates to cyclic alcohols. The reduction of substrates by SmBr<sub>2</sub>-NMEA that are typically recalcitrant to single-electron transfer demonstrates the potential of chelation-promoted bond weakening to achieve difficult chemical transformations.

## ASSOCIATED CONTENT

### Supporting Information

The Supporting Information is available free of charge at <https://pubs.acs.org/doi/10.1021/acs.inorgchem.3c00298>.

Experimental methods, spectroscopic, conductivity, and hydrogen gas evolution experiments, kinetics, <sup>1</sup>H and <sup>13</sup>C NMR data, and computational data (PDF)

## AUTHOR INFORMATION

### Corresponding Author

Robert A. Flowers, II – Department of Chemistry, Lehigh University, Bethlehem, Pennsylvania 18015, United States; [orcid.org/0000-0003-2295-1336](https://orcid.org/0000-0003-2295-1336); Email: [rof2@lehigh.edu](mailto:rof2@lehigh.edu)

### Authors

Nicholas G. Boekell – Department of Chemistry, Lehigh University, Bethlehem, Pennsylvania 18015, United States  
 Caroline O. Bartulovich – Department of Chemistry, Lehigh University, Bethlehem, Pennsylvania 18015, United States  
 Sandeepan Maity – Department of Chemistry, C. V. Raman Global University, Bhubaneswar, Odisha 752054, India

Complete contact information is available at: <https://pubs.acs.org/doi/10.1021/acs.inorgchem.3c00298>

## Notes

The authors declare no competing financial interest.

## ACKNOWLEDGMENTS

R.A.F.II gratefully acknowledges generous support by the National Science Foundation (CHE-1954892).

## REFERENCES

- Boekell, N. G.; Flowers, R. A. Coordination-Induced Bond Weakening. *Chem. Rev.* **2022**, *122*, 13447–13477.
- Brines, L. M.; Coggins, M. K.; Chaau, P.; Poon, Y.; Toledo, S.; Kaminsky, W.; Kirk, M. L.; Kovacs, J. A. Water-Soluble Fe(II)–H<sub>2</sub>O Complex with a Weak O–H Bond Transfers a Hydrogen Atom via an Observable Monomeric Fe(III)–OH. *J. Am. Chem. Soc.* **2015**, *137*, 2253–2264.
- Bezdek, M. J.; Guo, S.; Chirik, P. J. Coordination-Induced Weakening of Ammonia, Water, and Hydrazine X–H Bonds in a Molybdenum Complex. *Science* **2016**, *354*, 730–733.
- Chciuk, T. V.; Anderson, W. R.; Flowers, R. A. High-Affinity Proton Donors Promote Proton-Coupled Electron Transfer by Samarium Diiodide. *Angew. Chem., Int. Ed.* **2016**, *55*, 6033–6036.
- Paradas, M.; Campaña, A. G.; Jiménez, T.; Robles, R.; Oltra, J. E.; Buñ, E.; Justicia, J.; Cá, D. J.; Cuerva, J. M. Understanding the Exceptional Hydrogen-Atom Donor Characteristics of Water in Ti(III)-Mediated Free-Radical Chemistry. *J. Am. Chem. Soc.* **2010**, *132*, 12748–12756.
- Chalkley, M. J.; Oyala, P. H.; Peters, J. C. Cp\* Noninnocence Leads to a Remarkably Weak C–H Bond via Metallocene Protonation. *J. Am. Chem. Soc.* **2019**, *141*, 4721–4729.
- Drover, M. W.; Schild, D. J.; Oyala, P. H.; Peters, J. C. Snapshots of a Migrating H-Atom: Characterization of a Reactive Iron(III) Indenide Hydride and Its Nearly Isoenergetic Ring-Protonated Iron(I) Isomer. *Angew. Chem., Int. Ed.* **2019**, *58*, 15504–15511.
- Schild, D. J.; Drover, M. W.; Oyala, P. H.; Peters, J. C. Generating Potent C–H PCET Donors: Ligand-Induced Fe-to-Ring Proton Migration from a Cp\*Fe(III)–H Complex Demonstrates a Promising Strategy. *J. Am. Chem. Soc.* **2020**, *142*, 18963–18970.
- Tarantino, K. T.; Miller, D. C.; Callon, T. A.; Knowles, R. R. Bond-Weakening Catalysis: Conjugate Aminations Enabled by the Soft Homolysis of Strong N–H Bonds. *J. Am. Chem. Soc.* **2015**, *137*, 6440–6443.
- Gentry, E. C.; Knowles, R. R. Synthetic Applications of Proton-Coupled Electron Transfer. *Acc. Chem. Res.* **2016**, *49*, 1546–1556.
- Zhang, Y.-Q.; Jakoby, V.; Stainer, K.; Schmer, A.; Klare, S.; Bauer, M.; Grimme, S.; Cuerva, J. M.; Gansäuer, A. Amide-Substituted Titanocenes in Hydrogen-Atom-Transfer Catalysis. *Angew. Chem., Int. Ed.* **2016**, *55*, 1523–1526.
- Chciuk, T. V.; Flowers, R. A. Proton-Coupled Electron Transfer in the Reduction of Arenes by SmI<sub>2</sub>-Water Complexes. *J. Am. Chem. Soc.* **2015**, *137*, 11526–11531.
- Kolmar, S. S.; Mayer, J. M. SmI<sub>2</sub>(H<sub>2</sub>O)<sub>n</sub> Reduction of Electron Rich Enamines by Proton-Coupled Electron Transfer. *J. Am. Chem. Soc.* **2017**, *139*, 10687–10692.
- Chciuk, T. V.; Anderson, W. R.; Flowers, R. A. Interplay between Substrate and Proton Donor Coordination in Reductions of Carbonyls by SmI<sub>2</sub>-Water Through Proton-Coupled Electron-Transfer. *J. Am. Chem. Soc.* **2018**, *140*, 15342–15352.
- Szostak, M.; Fazakerley, N. J.; Parmar, D.; Procter, D. J. Cross-Coupling Reactions Using Samarium (II) Iodide. *Chem. Rev.* **2014**, *114*, 5959–6039.
- Ashida, Y.; Arashiba, K.; Nakajima, K.; Nishibayashi, Y. Molybdenum-Catalysed Ammonia Production with Samarium Diiodide and Alcohols or Water. *Nature* **2019**, *568*, 536–540.

- (17) Bartulovich, C. O.; Flowers, R. A. Coordination-Induced O-H Bond Weakening in Sm(II)-Water Complexes. *Dalt. Trans.* **2019**, *48*, 16129–16462.
- (18) Miller, R. S.; Sealy, J. M.; Shabangi, M.; Kuhlman, M. L.; Fuchs, J. R.; Flowers, R. A. Reactions of SmI<sub>2</sub> with Alkyl Halides and Ketones: Inner-Sphere vs Outer-Sphere Electron Transfer in Reactions of Sm(II) Reductants. *J. Am. Chem. Soc.* **2000**, *122*, 7718–7722.
- (19) Prasad, E.; Flowers, R. A. Reduction of Ketones and Alkyl Iodides by SmI<sub>2</sub> and Sm(II)-HMPA Complexes. Rate and Mechanistic Studies. *J. Am. Chem. Soc.* **2002**, *124*, 6895–6899.
- (20) Evans, W. J.; Bloom, I.; Hunter, W. E.; Atwood, J. L. Synthesis and X-Ray Crystal Structure of a Soluble Divalent Organosamarium Complex. *J. Am. Chem. Soc.* **1981**, *103*, 6507–6508.
- (21) Ramírez-Solís, A.; Bartulovich, C. O.; León-Pimentel, C. I.; Saint-Martin, H.; Boekell, N. G.; Flowers, R. A. Proton Donor Effects on the Reactivity of SmI<sub>2</sub>. Experimental and Theoretical Studies on Methanol Solvation vs. Aqueous Solvation. *Dalt. Trans.* **2020**, *49*, 7897–7902.
- (22) *Gaussian 09*, Revision D.01, Frisch, M. J.; Trucks, G. W.; Schlegel, H. B.; Scuseria, G. E.; Robb, M. A.; Cheeseman, J. R.; Scalmani, G.; Barone, V.; Mennucci, B.; Petersson, G. A.; Nakatsuji, H.; Caricato, M.; Li, X.; Hratchian, H. P.; Izmaylov, A. F.; Bloino, J.; Zheng, G.; Sonnenberg, J. L.; Hada, M.; Ehara, M.; Toyota, K.; Fukuda, R.; Hasegawa, J.; Ishida, M.; Nakajima, T.; Honda, Y.; Kitao, O.; Nakai, H.; Vreven, T.; Montgomery, J. A., Jr.; Peralta, J. E.; Ogliaro, F.; Bearpark, M.; Heyd, J. J.; Brothers, E.; Kudin, K. N.; Staroverov, V. N.; Kobayashi, R.; Normand, J.; Raghavachari, K.; Rendell, A.; Burant, J. C.; Iyengar, S. S.; Tomasi, J.; Cossi, M.; Rega, N.; Millam, J. M.; Klene, M.; Knox, J. E.; Cross, J. B.; Bakken, V.; Adamo, C.; Jaramillo, J.; Gomperts, R.; Stratmann, R. E.; Yazyev, O.; Austin, A. J.; Cammi, R.; Pomelli, C.; Ochterski, J. W.; Martin, R. L.; Morokuma, K.; Zakrzewski, V. G.; Voth, G. A.; Salvador, P.; Dannenberg, J. J.; Dapprich, S.; Daniels, A. D.; Farkas, Ö.; Foresman, J. B.; Ortiz, J. V.; Cioslowski, J.; Fox, D. J., Gaussian, Inc., Wallingford CT, 2013
- (23) Shotwell, J. B.; Sealy, J. M.; Flowers, R. A. Structure and Energetics of the Samarium Diiodide-HMPA Complex in Tetrahydrofuran. *J. Org. Chem.* **1999**, *64*, 5251–5255.
- (24) Maity, S.; Flowers, R. A.; Hoz, S. Aza versus Oxophilicity of SmI<sub>2</sub>: A Break of a Paradigm. *Chem. - A Eur. J.* **2017**, *23*, 17070–17077.
- (25) Duffy, L. A.; Matsubara, H.; Procter, D. J. A Ring Size-Selective Reduction of Lactones Using SmI<sub>2</sub> and H<sub>2</sub>O. *J. Am. Chem. Soc.* **2008**, *130*, 1136–1137.
- (26) Sautier, B.; Lyons, S. E.; Webb, M. R.; Procter, D. J. Radical Cyclization Cascades of Unsaturated Meldrum's Acid Derivatives. *Org. Lett.* **2012**, *14*, 146–149.
- (27) Guazzelli, G.; De Grazia, S.; Collins, K. D.; Matsubara, H.; Spain, M.; Procter, D. J. Selective Reductions of Cyclic 1,3-Diesters Using SmI<sub>2</sub> and H<sub>2</sub>O. *J. Am. Chem. Soc.* **2009**, *131*, 7214–7215.
- (28) Parmar, D.; Matsubara, H.; Price, K.; Spain, M.; Procter, D. J. Lactone Radical Cyclizations and Cyclization Cascades Mediated by SmI<sub>2</sub>-H<sub>2</sub>O. *J. Am. Chem. Soc.* **2012**, *134*, 12751–12757.
- (29) Chciuk, T. V.; Anderson, W. R.; Flowers, R. A. Proton-Coupled Electron Transfer in the Reduction of Carbonyls by Samarium Diiodide-Water Complexes. *J. Am. Chem. Soc.* **2016**, *138*, 8738–8741.
- (30) Morrill, C.; Péter, A.; Amalina, I.; Pye, E.; Crisenza, G. E. M.; Kaltsoyannis, N.; Procter, D. J. Diastereoselective Radical 1,4-Ester Migration: Radical Cyclizations of Acyclic Esters with SmI<sub>2</sub>. *J. Am. Chem. Soc.* **2022**, *144*, 13946–13952.
- (31) Hansen, A. M.; Lindsay, K. B.; Antharjanam, P. K. S.; Karaffa, J.; Daasbjerg, K.; Flowers, R. A., II; Skrydstrup, T. Mechanistic Evidence for Intermolecular Radical Carbonyl Additions Promoted by Samarium Diiodide. *J. Am. Chem. Soc.* **2006**, *128*, 9616–9617.
- (32) Venditto, N. J.; Liang, Y. S.; El Mokadem, R. K.; Nicewicz, D. A. Ketone-Olefin Coupling of Aliphatic and Aromatic Carbonyls Catalyzed by Excited-State Acridine Radicals. *J. Am. Chem. Soc.* **2022**, *144*, 11888–11896.
- (33) Boyd, E. A.; Peters, J. C. Sm(II)-Mediated Proton-Coupled Electron Transfer: Quantifying Very Weak N-H and O-H Homolytic Bond Strengths and Factors Controlling Them. *J. Am. Chem. Soc.* **2022**, *144*, 21337–21346.
- (34) Dahlén, A.; Hilmersson, G.; Knettle, B. W.; Flowers, R. A. Rapid SmI<sub>2</sub>-Mediated Reductions of Alkyl Halides and Electrochemical Properties of SmI<sub>2</sub>/H<sub>2</sub>O/Amine. *J. Org. Chem.* **2003**, *68*, 4870–4875.
- (35) Dahlén, A.; Hilmersson, G. Mechanistic Study of the SmI<sub>2</sub>/H<sub>2</sub>O/Amine-Mediated Reduction of Alkyl Halides: Amine Base Strength (PKBH<sup>+</sup>) Dependent Rate. *J. Am. Chem. Soc.* **2005**, *127*, 8340–8347.
- (36) Maity, S.; Hoz, S. Deciphering a 20-Year-Old Conundrum: The Mechanisms of Reduction by the Water/Amine/SmI<sub>2</sub> Mixture. *Chem. - A Eur. J.* **2015**, *21*, 18394–18400.